Solar Energy Materials & Solar Cells 94 (2010) 629–633

Contents lists available at ScienceDirect

Solar Energy Materials & Solar Cells

journal homepage: www.elsevier.com/locate/solmat

Letter

Enhancement of the light conversion efficiency of silicon solar cells by using nanoimprint anti-reflection layer

J.Y. Chen, K.W. Sun *

Department of Applied Chemistry, National Chiao Tung University, Hsinchu, Taiwan

ARTICLE INFO

Article history:
Received 23 September 2009
Accepted 26 November 2009
Available online 22 December 2009

Keywords:
Nanoimprint
Anti-reflection
Sub-wavelength structure

ABSTRACT

In this report, the results of the fabrication of nanostructured Si molds by e-beam lithography and chemical wet etching are presented. A home-made pneumatic nanoimprint system was used to transfer the mold patterns to a PMMA layer on a Si template using the spin-coating replication/hot-embossing techniques. The patterned PMMA layer was peeled off from the Si template and directly transferred onto the surface of a poly-Si P–N junction solar cell device to serve as the anti-reflection (AR) layer. It provides a simple and low-cost means for large-scale use in the production of AR layers for improving solar cell performance. A drastic reduction in reflectivity of the AR layer over a broad spectral range was demonstrated. In addition, the great improvement on the light harvest efficiency of the solar cells from 10.4% to 13.5% using the nanostructured PMMA layer as the AR layer was validated.

1. Introduction

An anti-reflection (AR) layer is a type of coating applied to the surface of a material to reduce light reflection and to increase light transmission. The AR layers can be used in the solar cell, planar displays, glasses, prisms, videos, and camera monitors. Surface-relief gratings with the size smaller than the wavelength of light, named sub-wavelength structure (SWS), behave as anti-reflection surfaces. By using a mechanically continuous wavelike grating (e.g., pyramidal, triangular, conical shapes), the SWS grating acts as a surface possessing a gradually and continuously changing refractive index profile from the air to the substrate. Deeper SWS grating can greatly enhance the anti-reflection effect, since the refractive index value changes smoothly and continuously. Tapered SWSs have been fabricated through different methods [1–3]. Ishimori et al. used an e-beam lithography technique to generate triangular structures in the photoresist and utilized a focused SF_6 fast atom beam (FAB) to produce tapered sub-wavelength structures. However, the fabrication costs, which involve either electron-beam lithography or various etching processes, can be significant. Recently, versatile SWSs have emerged as promising candidates for AR coatings such as etching with self-aggregated nanodot mask [4,5], moth-eye like fabrication [6,7], nanorod fabrication [8–10], and nanostructures employing oblique-angle deposition methods [11,12].

Nanoimprint lithography (NIL), which was first demonstrated by Chou et al. [13], is a lithography technique performed by pressing the patterned mold so that it makes contact with the polymer resist directly. The patterns on the mold will transfer to the polymer resist without any exposure source. Therefore, the diffraction effect of light can be ignored and limitation is dependent only on the pattern size of mold rather than the wavelength of exposure light. This technology provides a different way to fabricate nanostructures with easy processes, high throughput, and low cost. It is capable of replicating patterns with a linewidth below 10 nm in a parallel manner [14]. NIL has been used to produce large-area polymer sheets with SWS as AR layers [15,16]. Most of the research presented good anti-reflection properties with the imprinted polymer layers. However, there is no report on the fabrication, nor tests of the properties of the real Si P–N junction solar cell devices incorporated with the nanoimprinted SWS as the AR layers. In this paper, we combined the NIL technology with solar cell devices and provided a promising technique for the fabrication of high efficiency solar cell.

2. Material and methods

The flow charts of the mold fabrication and spin-coating replication/hot-embossing NIL processes are shown in Fig. 1. A silicon wafer was used as the substrate for the hot-embossing NIL mold fabrication. The substrate surface was first cleaned up with ACE, IPA, and D.I. water by ultrasonic agitation. A 50 nm SiO_2 was deposited on the surface as the mask of the wet etching. The sample was then coated with ZEP-520A photoresist and exposed to the electron beam (Elionix ELS-7500EX 50 kV Electron Beam Lithography

* Corresponding author.
E-mail address: kwsun@mail.nctu.edu.tw (K.W. Sun).

0927-0248/$ - see front matter © 2009 Elsevier B.V. All rights reserved.
doi:10.1016/j.solmat.2009.11.028

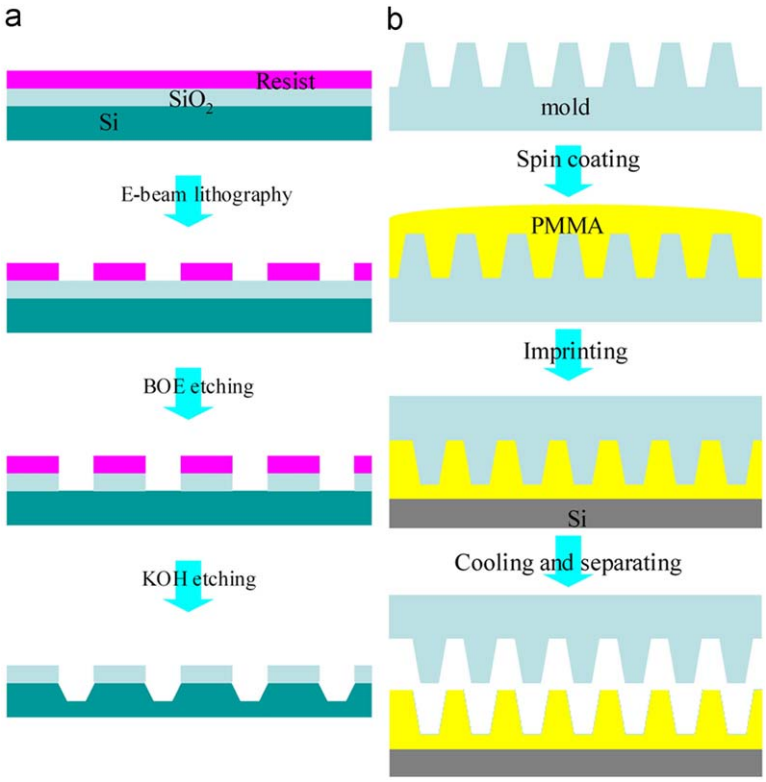

Fig. 1. Steps used for (a) the mold fabrication and (b) the spin-coating replication/hot-embossing processes.

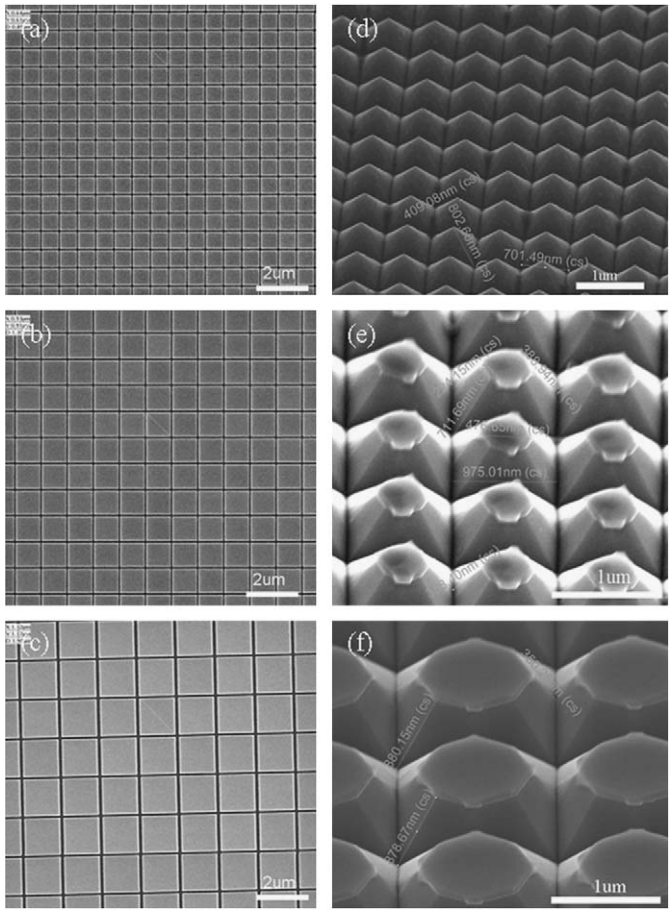

Fig. 2. SEM images of the e-beam defined grating patterns with pitches of (a) 700 nm (b) 1000 nm and (c) 1500 nm. SEM images of the fabricated silicon molds with pitches of (d) 700 nm (e) 1000 nm and (f) 1500 nm.

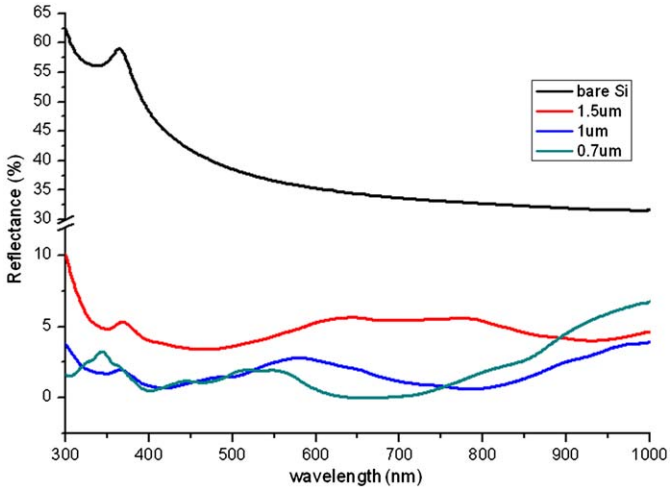

Fig. 3. Reflection spectra of the fabricated silicon molds with different pitches and bare Si.

system). 2D patterns within a square area measuring 5 mm by 5 mm, as shown in Fig. 2(a)–(c), were defined on the mold surface with a linewidth of 80 nm and pitches of 700, 1000, and 1500 nm, respectively. After developing with ZED-N50, the e-beam defined patterns were first chemically etched in a solution mixture of HF and NH_4F (1:6) for 15 s to transfer the pattern on the SiO_2 mask. Then, the entire mold was dipped into KOH solution mixture with 30% KOH and 20% IPA for 1–5 min at 80 °C. Due to the transverse etching of the acid solution and the anisotropic etching of KOH solution, the wet etching process resulted in different tapered nano-post arrays as shown in Fig. 2(d)–(f). For the mold with 700 nm pitch, the nanostructures have a tapered angle cone shape with a square base. However, for the mold with pitches of 1000 and 1500 nm, the structures formed octagonal-shaped cones with a flat top. The depths of the three molds were all near 700–900 nm. The reflection spectra of the molds, as shown in Fig. 3, were measured by an n&k analyzer (n&k technology, Inc./n&k analyzer 1280) for wavelengths that ranged from 300 to 1000 nm. Spectra of all molds showed significantly reduced reflectance ($<6\%$) through the entire wavelength range at normal incidence. The mold with a period of 700 nm shows the lowest reflectivity among the three due to its tapered angle cone shape [1–3]. The processes of transferring the patterns on the mold to the solar cells are given as follows.

The spin-coating replication/hot-embossing techniques and a home-made pneumatic nanoimprintor were used to transfer the patterns on the molds to a PMMA layer on a Si template. Before the imprinting processes, the mold was first placed in a closed bottle filled with vaporized 1H,1H,2H,2H-perfluoro-octyltrichlorosilane at 250 °C for 1 hr. The mold release agent coated on the mold can facilitate the separation of the replica from the mold after the imprinting process. A layer of PMMA of 950 K molecular weight and solid contents of 15% in anisole was spin-coated on the mold at 1000 rpm. The substrate and mold were then combined and placed on the sample stage in our home-made nanoimprintor. The PMMA films were hot-embossed at a temperature of 120 °C under a pressure of 0.4 kg/cm^2. The pressure was relieved and the sample was de-molded after the stage has cooled down to room temperature.

3. Results and discussion

The resulting patterns on the PMMA layers after the imprinting processes are shown in Fig. 4(a)–(c). The nanostructures after the

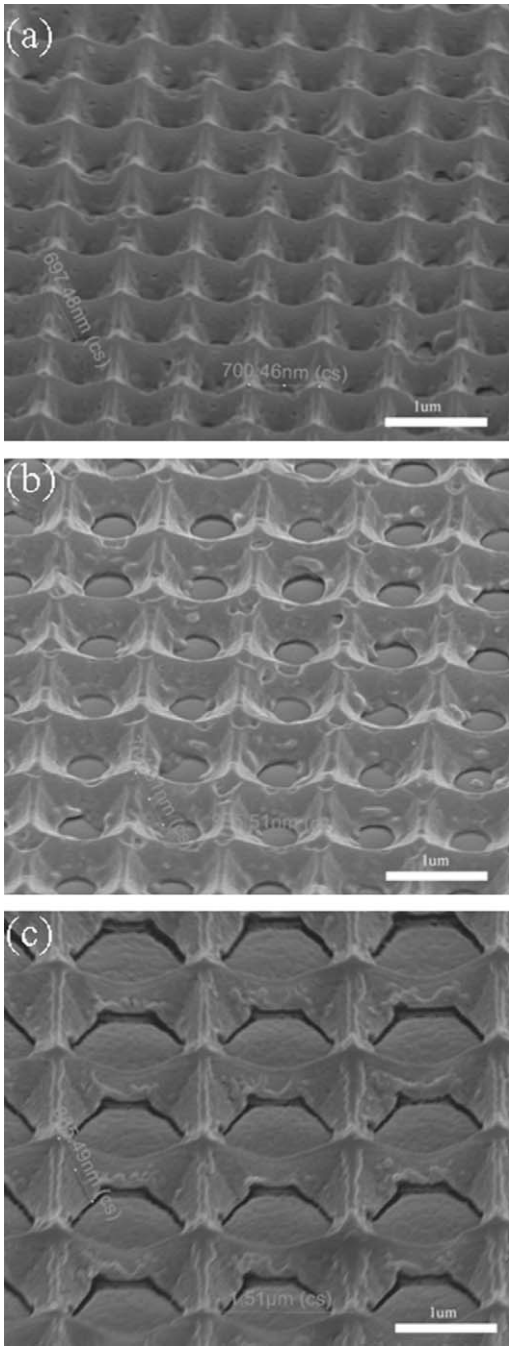

Fig. 4. SEM images of the replicated PMMA sub-wavelength structures with pitches of (a) 700 nm (b) 1000 nm and (c) 1500 nm.

NIL have the same depth as the molds. The ability of the PMMA to fill completely the molds when it was spin-coated on the mold accounts for this. In Fig. 5(a), the reflectance spectra and the comparisons of AR performance of the nanostructured PMMA layers with bare Si are shown. In contrast to the AR measurements from the molds, the nanostructured PMMA layer formed by the mold with a pitch of 1500 nm now has the lowest reflectivity for the entire wavelength range. In general, the tapered cone structure with a very steep angle and a polygon base can lead to the gradually and continuously change of the refractive index profile from the air to the substrate [1–3]. Therefore, it can greatly reduce the reflection from the surface. That is why the nanostructured Si mold with period of 700 nm (as shown in Fig. 3) has the lowest reflectivity. However, after the imprint

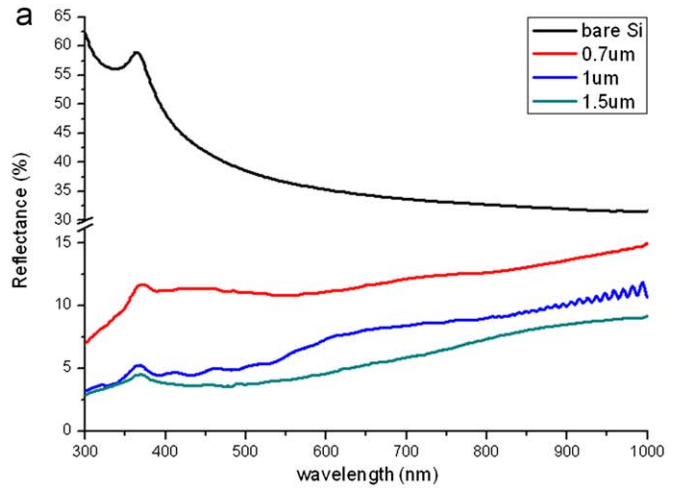

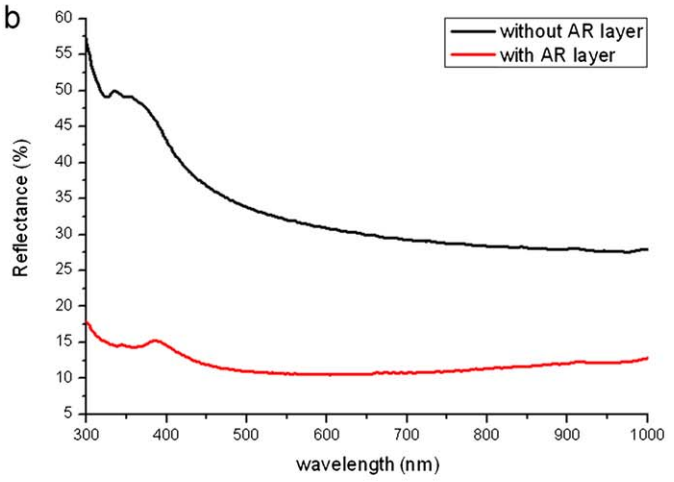

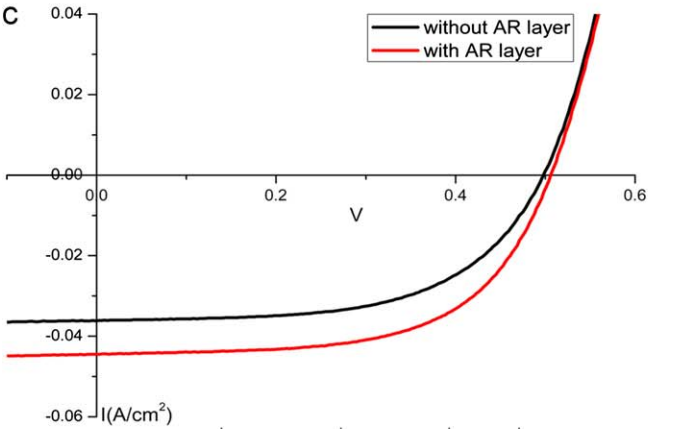

	V_{OC}(V)	I_{SC}(mA)	FF	η (%)
Without AR layer	0.50	36.2	0.57	10.4
With AR layer	0.51	44.5	0.59	13.5

Fig. 5. (a) Reflection spectra of the replicated PMMA sub-wavelength structures with different pitches and bare Si. (b) Reflection spectra of the poly-Si P–N junction solar cells with and without the nanostructured PMMA layer with a pitch size of 1500 nm. (c) Current–voltage characteristics, fill factor, and conversion efficiency of the solar cells with and without the nanostructured PMMA layer.

processes, the nanostructured PMMA layer with a pitch of 1500 nm (as shown in Fig. 4(c)) now has a more significant tapered cone shape in compared to the PMMA layer with the pitch of 700 nm, which has a much less sharp tapered structure (as shown in Fig. 4(a)).

Finally, the PMMA layers were peeled off from the Si templates and directly transferred onto the poly-Si solar cell surface. In this work, the solar cells were fabricated on boron-doped poly-Si substrates with a thickness of 200 μm. The substrate was first doped to n-type with Centrothem E-2000 APCVD. The ion implanting depth was 80 nm. After the dopant activation, the top and backside contacts were formed by a printer system (Baccini screen printing line) with Ag and Al. Finally, the cell was annealed at 850 °C to form Ohmic contacts on both sides. It should be noted that, due to the metal contact on the cell, the PMMA thin film could not completely sit flat on the surface. The reflectivity of the PMMA film on the solar cells was increased slightly than when sitting on a flat surface [see Fig. 5(b)]. The poly-Si solar cell with PMMA thin film was characterized under the Air mass 1.5 global (AM 1.5G) illumination condition and was compared to the cell that did not undergo the anti-reflection treatment. The measured current–voltage characteristics are shown in Fig. 5(c). The short-circuit current was enhanced by 23% due to the PMMA nanostructured film. The light conversion efficiency of the solar cells was improved from 10.4% to 13.5% with the use of PMMA thin film as the AR layer.

4. Conclusions

In summary, we present a simple and low-cost method to produce polymer sheets with 2D periodic structures using the spin-coating replication/hot-embossing nanoimprint lithography, lift-off, and direct transfer techniques. The structures can reduce surface Fresnel reflection over a broad spectral range. This technology was used for AR applications in solar cells for improving their light conversion efficiency. The light harvest efficiency of the poly-Si solar cells was improved by over 30% with the AR layers. It can find applications in other electro-optical devices.

Acknowledgements

This work was supported by the National Science Council of Republic of China under contract no. NSC 96-2112-M-009- 024 –MY3, NSC 96-2120-M-009-004-, and the MOE ATU program.

References

[1] M. Ishimori, Y. Kanamori, M. Sasaki, K. Hane, Subwavelength antireflection gratings for light emitting diodes and photodiodes fabricated by fast atom beam etching, Jpn. J. Appl. Phys. vol. 41 (2002) 4346–4349.
[2] Y. Kanamori, M. Sasaki, K. Hane, Broadband antireflection gratings fabricated upon silicon substrates, Opt. Lett. 24 (1999) 1422–1424.
[3] K. Hadobas, S. Kirsch, A. Carl, M. Acet, E.F. Wassermann, Reflection properties of nanostructure-arrayed silicon surfaces, Nanotechnology 11 (2000) 161–164.
[4] S. Wang, X.Z. Yu, H.T. Fan, Simple lithographic approach for subwavelength structure antireflection, Appl. Phys. Lett. 91 (2007) 061105–061107.
[5] G.-R. Lin, Y.-C. Chang, E.-S. Liu, H.-C. Kuo, H.-S. Lin, Low refractive index Si nanopillars on Si substrate, Appl. Phys. Lett. 90 (2007) 181923–181925.
[6] C.-H. Sun, W.-L. Min, N.C. Linn, P. Jiang, B. Jiang, Templated fabrication of large area subwavelength antireflection gratings on silicon, Appl. Phys. Lett. 91 (2007) 231105–231107.
[7] C.-H. Sun, P. Jiang, B. Jiang, Broadband moth-eye antireflection coatings on silicon, Appl. Phys. Lett. 92 (2008) 061112–061114.
[8] Y.-J. Lee, D.S. Ruby, D.W. Peters, B.B. McKenzie, J.W.P. Hsu, ZnO nanostructures as efficient antireflection layers in solar cells, Nano. Lett. 8 (2008) 1501–1505.
[9] T.H. Ghong, Y.D. Kim, E. Ahn, E. Yoon, S.J. An, G.–C. Yi, Application of spectral reflectance to the monitoring of ZnO nanorod growth, Appl. Surf. Sci. 255 (2008) 746–748.
[10] Z. Wang, B. Huang, X. Qin, X. Zhang, P. Wang, J. Wei, J. Zhan, X. Jing, H. Liu, Z. Xu, H. Cheng, X. Wang, Z. Zheng, Growth of high transmittance vertical aligned ZnO nanorod arrays with polyvinyl alcohol by hydrothermal method, Mater. Lett. 63 (2009) 130–132.

[11] M.-L. Kuo, D.J. Poxson, Y.S. Kim, F.W. Mont, J.K. Kim, E.F. Schubert, S.-Y. Lin, Realization of a near-perfect antireflection coating for silicon solar energy utilization, Opt. Lett. 33 (2008) 2527–2529.
[12] P. Yu, C.-H. Chang, C.-H. Chiu, C.-S. Yang, J.-C. Yu, H.-C. Kuo, S.-H. Hsu, Y.-C. Chang, Efficiency enhancement of GaAs photovoltaics employing antireflective indium tin oxide nanocolumns, Adv. Mater. 21 (2009) 1618–1621.
[13] S.Y. Chou, P.R. Krauss, J. Renstrom, Imprint of sub-25 nm vias and trenches in polymers, Appl. Phys. Lett 67 (1995) 3114–3116.
[14] V. Boerner, S. Abbott, B. Blasi, A. Gombert, W. Hobfeld, Holographyic antiglare and antireflection film for flat panel displays, SID Symp. Digest. 34 (2003) 68–71.
[15] C.-J. Ting, M.-C. Huang, H.-Y. Tsai, C.-P. Chou, C.-C. Fu, Low cost fabrication of the large-area anti-reflection films from polymer by nanoimprint/hot-embossing technology, Nanotechnology 19 (2008) 205301–205305.
[16] Y. Kanamori, E. Roy, Y. Chen, Antireflection sub-wavelength gratings fabricated by spin-coating replication, Microelectron. Eng. 78-79 (2005) 287–293.